

Linear Depth Stabilizer and Quantum Fourier Transformation Circuits with no Auxiliary Qubits in Finite Neighbor Quantum Architectures

Dmitri Maslov
Institute for Quantum Computing,
University of Waterloo, Waterloo, ON, Canada,
N2L 3G1. Email: dmitri.maslov@gmail.com.

(Dated: November 4, 2018)

In this paper we investigate how quantum architectures affect the efficiency of the execution of the Quantum Fourier Transform (QFT) and linear transformations, which are essential parts of the stabilizer/Clifford group circuits. In particular, we show that in most common and realistic physical architectures including Linear Nearest Neighbor (LNN), 2D lattice, and bounded degree graph (containing a chain of length n), n -qubit QFT and n -qubit stabilizer circuits can be parallelized to linear depth using no auxiliary qubits. We construct lower bounds that show the efficiency of our approach.

PACS numbers: 03.67.Lx, 03.67.Pp

I. INTRODUCTION

Quantum computation has attracted attention because it appears to reduce the computational complexity of certain calculations, see, for example, [1, 2]. For the quantum circuit model of computation, there exists a number of physical quantum information processing implementations, such as liquid NMR (up to 12 qubits at a time) [3], and trapped ions (8 qubits) [4]. Generally, a large number of qubits is required for computational purposes. In this work, we do not allow for any auxiliary qubits to be used in order to reflect the apparent hardness of scaling up quantum information processing devices.

Quantum circuits have been optimized to require less space, fewer gates and smaller depth. This is important from the point of view of the efficient potential realization of the quantum algorithms. As discussed in the first paragraph, we address the issue of space minimization by restricting the number of auxiliary qubits to zero. Our next focus is on depth minimization. This is because a small depth circuit does not only mean a fast computation, but also helps reduce the effect of decoherence. For instance, it is possible to construct realistic examples in which a smaller depth circuit will require fewer levels of error correction, and each error correction code concatenation step is a very expensive operation [5].

In this paper, the depth of a circuit is defined as the number of logic levels in it. Each logic level is a set of non-intersecting “elementary” gates. It is generally accepted that in a practical quantum information processing approach, it should be possible to execute independent gates in parallel. The gate libraries considered in the relevant literature include a set of single-qubit and CNOT gates (which is most likely an artifact of the well known result showing the completeness of this gate set, however, CNOT may not necessarily be a natural gate for some quantum information processing proposals), and any two-qubit operation. Indeed, given a Hamiltonian, any two-qubit operation can be efficiently implemented [6]. For the sake of completeness, this paper discusses how the results apply to both gate sets. Circuit depth, as defined above, upper bounds a possibly lower circuit runtime in cases when next logic level can be executed based upon the availability

of qubits and before execution of the gates from the previous level has completed. Practically, this means that some of our upper bounds may not be tight (which is advantageous in the sense that the implementation we construct may in fact have a smaller runtime than predicted by the formulas evaluating depth).

Quantum algorithms and their circuits are usually formulated without considering the physical limitations imposed by different architectures. We believe that circuit and algorithm designs need to be modified to account for possible architectures. In particular, in realistic architectures, it is not possible to establish direct interactions between every pair of qubits [3, 4, 7]. A study of quantum computing architectures for the existing and emerging quantum technologies shows that the fastest possible direct interactions form a bounded degree graph (e.g., liquid NMR quantum information processing), and 1D or 2D (sub)lattices [8]. A mixed architecture, where values of stationary qubits may be teleported with the help of flying qubits to where they are desired was studied in [9]. In this work, the role of stationary qubits is played by the spins of phosphorus atoms embedded in silicon, known as the Kane proposal [10], and the flying qubits are photons, with the information being teleported via EPR states. Other proposals for state transfer between either stationary or both flying and stationary qubits, and discussions of mixed architectures, can be found, for example, in [11, 12, 13] and the references therein. However, an architecture that allows interconversion between stationary and flying qubits cannot in general be realized in any technology. In addition, it was shown that teleportation of a *single* value (simultaneous teleportation of many qubits may be less efficient) in the Kane architecture is only efficient if compared to *more* than 2-4 levels of SWAPs [9]. A similar effect is likely to take place in other mixed architecture proposals. The latter is important for this work since we are only using depth-1 swapping of multiple qubits via SWAP gates.

Generally speaking, due to the spatial constraints it seems unrealistic to believe that a direct scalable implementation of the unrestricted (where every two qubits are neighbors) architecture, or, more generally, unbounded neighbor architecture, will ever be found. Furthermore, in classical computation the

number of neighbors is limited, and there is no obvious reason to believe that the quantum world is different. Thus, the complexity of the circuit designs must be refined to take into account the limitations of possible quantum computing architectures.

The linear nearest neighbor (LNN) architecture, also known as chain nearest neighbor, is often considered as a good (and, in fact, very restrictive) approximation to what a scalable quantum architecture may be. Mathematically, in an LNN architecture with n qubits q_1, q_2, \dots, q_n , two-qubit gates are allowed between any qubits whose subscript values differ by one. The LNN architecture describes 1D lattices. It misses possible direct interactions in 2D lattices and may restrict the number of useful interactions in connected graphs. However, if one can show that a circuit can be efficiently reorganized to be executed in the LNN architecture, such a circuit could be run efficiently in many other architectures.

The Quantum Fourier Transformation (QFT) is an analogue of the classical discrete Fourier transformation, however, in the quantum case the transformation is applied to the amplitudes. The QFT serves as a basis for a number of efficient quantum algorithms. Most notably, it is at the heart of integer factorization and the discrete logarithm polynomial time quantum algorithms [2]. Therefore, efficient implementation of the QFT is important. This is why this topic has been studied extensively [14, 15, 16]. Researchers presented linear and logarithmic depth circuits using a number of auxiliary qubits. Known circuits for the QFT have a regular structure [5, 16]. However, they require direct interaction between every two qubits, which makes such circuits especially inconvenient for quantum architectures where only a finite number of neighbors is allowed. In an architecture with a finite number of neighbors, such as LNN, state transfer down the chain may require up to $(n-1)$ SWAP gates. We refer to this observation as the *locality constraint* in the discussions involving lower bound arguments. A linear depth QFT circuit implemented in the LNN architecture has been reported in [17]. We reconstruct this circuit with our generalized technique and we also study lower bounds.

Stabilizer circuits (also known as unitary stabilizer circuits or Clifford group circuits) were introduced and studied for their use in the encoding, decoding and error detection stages of quantum error-correction codes [18, 19]. They can be defined as arbitrary quantum circuits composed with single-qubit Hadamard and Phase gates and two-qubit controlled-NOT gates. It turns out that stabilizer circuits can be efficiently simulated [20] as an 11-stage sequence of Hadamard (H), Phase (P) and linear reversible circuits (C) as H-C-P-C-P-C-H-P-C-P-C. Each P and H stage is a depth-1 computation composed with single-qubit gates. The depth of stabilizer circuits is, thus, defined by the depth of a circuit realizing some linear reversible function. Efficient circuits for linear functions are, therefore, of great importance. In this paper we show that every stage C can be parallelized to linear depth in the LNN architecture. Thus, the entire stabilizer circuit requires at most linear time to be executed.

A very recent study shows that a size s stabilizer circuit in an *unrestricted* architecture can be parallelized to a depth

$O(\log n)$ circuit, but requires $O(s^3 + n)$ auxiliary qubits [21], Proposition 8.9. Combining the results of [20, 21, 22] this gives a depth $O(\log n)$ circuit in unrestricted architectures using $O(\frac{n^6}{\log^3 n})$ auxiliary qubits to realize any stabilizer circuit. Since a depth d circuit built on q qubits in unrestricted architectures may become as large as depth $O(qd)$ in the LNN architecture (every depth-2 computation can be adversary made to define the complete interaction pattern of the LNN architecture, and two depth-2 non-commuting stages can be defined such as to require a linear depth qubit permutation between them), the benefit of logarithmic depth quickly disappears. However, a large amount of auxiliary qubits remains. Our approach thus appears more practical.

The remainder of the paper is organized as follows. We start by introducing a concept of skeleton circuits and studying their properties. In Subsections II A and II B the lessons learned are applied to show that QFT and linear reversible/stabilizer circuits can be parallelized to linear depth in the LNN architecture. Section III reports lower bounds for a class of skeleton circuits which appears to be very important. Concluding remarks can be found in Section IV.

II. SKELETON CIRCUITS

Any quantum circuit composed with single-qubit and two-qubit gates can be thought of as a circuit composed of generic two-qubit operations each of which consists of a two-qubit gate of the initial circuit with the surrounding gates absorbed into it (the trivial case when only single-qubit gates are applied to a specific qubit throughout an entire computation is ignored as not interesting). We call this a *skeleton circuit*. Obviously, the complexity of a skeleton circuit defines the complexity of the initial circuit (assuming that any two-qubit gate has a finite cost) and vice versa. We next study skeleton circuits of a certain type and apply the lessons learned to construct circuits for QFT and linear reversible/stabilizer circuits of linear depth in the LNN architecture.

The basic skeleton circuit we consider is illustrated in Fig. 1(a). Mathematically, the skeleton circuit SC is defined as

$$SC := G_1^{i_1}(q_1, q_2) G_2^{i_2}(q_1, q_3) \dots G_{n-1}^{i_{n-1}}(q_1, q_n) \\ G_n^{i_n}(q_2, q_3) \dots G_{n(n-1)/2}^{i_{n(n-1)/2}}(q_{n-1}, q_n), \quad (1)$$

where G_* ($*$ is reserved to represent any possible existing value of subscript) is a two-qubit gate that operates on the qubits indicated in brackets, i_* take Boolean values, and for a gate G , G^1 is the gate G itself, whereas $G^0 = Id$ (identity, *i.e.*, this gate is not applied). In other words, i_* are used to indicate whether a gate is present or not.

Since all quantum gates that operate on non-intersecting sets of qubits commute, the SC circuit can be executed in parallel in $(2n-3)$ computational stages $L_1, L_2, \dots, L_{2n-3}$ defined as follows: $L_1 := G_1^{i_1}$, $L_2 := G_2^{i_2}$, $L_3 := G_3^{i_3} G_n^{i_n}$, $L_4 := G_4^{i_4} G_{n+1}^{i_{n+1}}$, $L_5 := G_5^{i_5} G_{n+2}^{i_{n+2}} G_{2n-2}^{i_{2n-2}}, \dots, L_{2n-3} := G_{n(n-1)/2}^{i_{n(n-1)/2}}$. This is illustrated in Fig. 1(b) in the case $n = 5$.

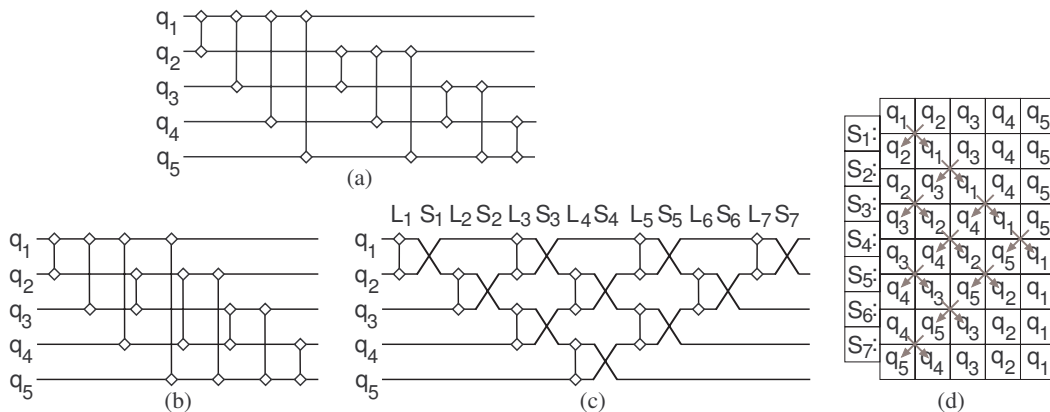


FIG. 1: Reorganizing an n -qubit skeleton circuit, illustrated for $n = 5$. (a) Original circuit with at most $\frac{n(n-1)}{2}$ gates. Each of the gates in this skeleton circuit may or may not be present. (b) Linear $(2n - 3)$ depth circuit possible to run in the “sea-of-qubits” architecture. (c) Version of (b) ready for execution in the LNN architecture. (d) This table illustrates how swapping stages S_* are constructed and inserted between the computational stages L_* .

Next, the circuit can be adapted to the LNN architecture through inserting SWAP gates $\text{SWAP}(q_s, q_t)$ after each gate $G_k^{i_k}(q_s, q_t)$. This is illustrated in Fig. 1(c) and (d) in the case $n = 5$. In the gate library containing all possible 2-qubit unitaries, the upper bound for depth is $(2n - 3)$. We next use this result to achieve linear depth circuits for QFT and stabilizer circuits. These are fairly tight upper bounds. With the best known asymptotic result requiring $\Theta(n^2)$ gates for the QFT, it can be shown that QFT cannot be computed in less than linear depth even in an unrestricted architecture. A counting argument applied to linear circuits [22] shows that there exists a stabilizer circuit that requires at least $\Theta(\frac{n^2}{\log n})$ gates, meaning that it is impossible to find a circuit for it with depth less than $\Theta(\frac{n}{\log n})$ even if the architecture is unrestricted. Lower bounds in restricted architectures (all of which turn out to be linear, and thus having the same asymptotic as the upper bound that follows from our construction) are studied in Section III.

Let us note that the skeleton circuit that we consider can be parallelized to linear depth in the LNN architecture for any initial permutation of the input and return the output in any desired order. For that, at most a linear depth swapping stage before and after the circuit is required, which does not change the overall linearity of the depth. The circuit illustrated in Fig. 1(c) not only allows execution in the LNN architecture, it also does not change the LNN connectivity pattern $(q_1 - q_2 - \dots - q_n)$, and thus such circuits can be applied one after the other with no swapping in between. This observation will be used in Subsection IIB. If the circuit in Fig. 1(c) is the last computational stage before the measurement is done, the last SWAP need not be applied.

A. QFT in the LNN architecture

A circuit that realizes the QFT and requires no ancilla qubits is illustrated in Fig. 2(a). Its skeleton circuit (Fig.

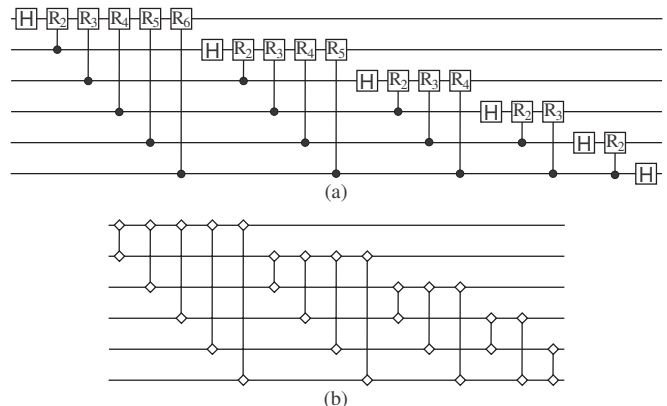


FIG. 2: (a) Circuit for n -qubit QFT [5], page 219, illustrated for $n = 6$. The two-qubit gates are controlled- Z rotations with parameter $1/2^k$, where k is the subscript in the gate notation. The single-qubit gates are Hadamard gates. (b) Skeleton circuit of the QFT circuit in (a) composed of generic two-qubit gates.

2(b)) is obviously of the type considered in the previous section with all $i_* = 1$. Therefore, the QFT can be parallelized to linear depth. This is, however, a known result, as [17] reports a construction that is equivalent to ours. It can also be observed that the approximate QFT circuit, where controlled rotations of the QFT circuit with small parameters are ignored, may be executed in linear depth in the LNN architecture. Lower bounds are discussed in Section III, and they apply directly to the QFT circuit.

B. Stabilizer/linear circuits

Synthesis of efficient linear circuits has been studied in [22]. The authors report a synthesis algorithm capable of pro-

ducing a circuit with $O(\frac{n^2}{\log n})$ CNOT gates. It was also proven that their synthesis is asymptotically optimal in that there exists a linear function that requires $\Theta(\frac{n^2}{\log n})$ CNOT gates. In this paper, the goal is different. We target minimization of the depth as opposed to the number of gates used. The depth of our circuit is linear in the number of qubits n , and it is upper bounded by $18n + O(1)$ CNOTs (assuming every SWAP is substituted with a suitable 3-CNOT implementation) or $6n + O(1)$ generic two-qubit gates. We also prove asymptotic optimality, which in our case is straightforward.

Every reversible linear function of n variables $\vec{q} = (q_1, q_2, \dots, q_n)^t$ can be written as matrix multiplication $A\vec{q}$, where A is an $n \times n$ Boolean non-singular matrix. Synthesizing such a function is equivalent to composing a sequence of gate operations that transforms matrix A into its reduced echelon form. Due to reversibility, the reduced echelon form of A is the identity matrix. A standard technique for transforming a matrix A to the identity is to apply the Gauss-Jordan elimination algorithm. In the following, we illustrate the application of the Gauss-Jordan elimination algorithm and then modify its circuit to allow it be executed with a linear number of computational stages. Parameters i_* and p_* take Boolean values and they are used to indicate whether the gate has been applied (1) or not (0). Parameters p_* are reserved for the gates applied to update values of the diagonal elements of the matrix A during Gauss-Jordan elimination.

- Step 1. Make sure that the pivot element $a_{1,1} \neq 0$. If $a_{1,1} \neq 0$ assign $p_1 := 0$. Otherwise choose $a_{j,1} \neq 0$, apply gate $\text{CNOT}(q_j, q_1)$ and make assignment $p_1 := 1$.
- Steps $s = 2..n$. Transform each $a_{s,1}$ to 0 through application (if needed) of the gate $\text{CNOT}(q_1, q_s)$. If at step s a gate was applied set $i_s := 1$, otherwise, $i_s := 0$.
- Step $n+1$. Make sure that the pivot element $a_{2,2} \neq 0$. If $a_{2,2} \neq 0$ do nothing ($p_2 := 0$), otherwise choose $a_{j,2} \neq 0$, apply gate $\text{CNOT}(q_j, q_2)$ and set $p_2 := 1$.
- Steps $s = (n+2)..(2n-1)$. Transform each $a_{s,2}$ to 0 through application (if needed) of the gate $\text{CNOT}(q_2, q_{s-n+1})$. If at step s a gate was applied set $i_s := 1$, otherwise, $i_s := 0$.
- ...
- Step $\frac{n(n+1)}{2} - 2$. Make sure that the pivot element $a_{n-1, n-1} \neq 0$. If $a_{n-1, n-1} \neq 0$ do nothing ($p_{n-1} := 0$), otherwise apply gate $\text{CNOT}(q_n, q_{n-1})$ and make assignment $p_{n-1} := 1$. After this step, all parameters p_* must be set.
- Step $\frac{n(n+1)}{2} - 1$. Transform each $a_{n, n-1}$ to 0 through application (if needed) of the gate $\text{CNOT}(q_{n-1}, q_n)$. If the gate was applied set $i_{\frac{n(n+1)}{2} - 1} := 1$, otherwise, $i_{\frac{n(n+1)}{2} - 1} := 0$. At this point, the set of applied transformations reduced matrix A to the upper triangular form with ones on diagonal. The remainder of the algorithm eliminates non-zero elements above the diagonal.

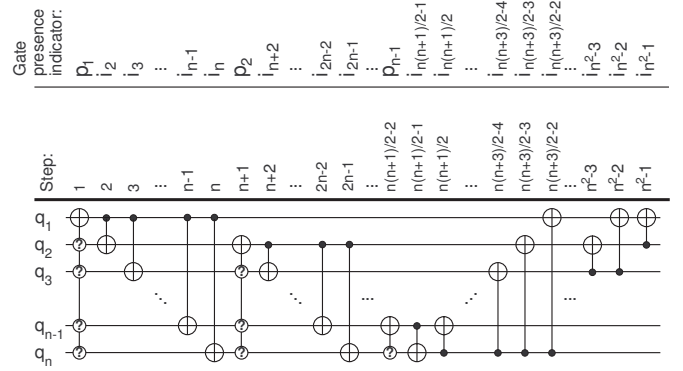


FIG. 3: Application of Gauss-Jordan elimination algorithm to the synthesis of a reversible network. Gates with controls $\textcircled{?}$ indicate a single CNOT each with the control at (exactly) one of positions marked $\textcircled{?}$.

- Steps $s = \frac{n(n+1)}{2}..(n^2-1)$. If $a_{k,l} \neq 0$, apply $\text{CNOT}(q_l, q_k)$ for $k = l..1$ inside for $l = n..2$ and set i_s to one iff a gate has been applied.

We next use the gate commutation rule (two CNOT gates commute iff target of one gate is not equal to the control of the other) and circuit identity $\text{CNOT}(a,c)\text{CNOT}(c,b) = \text{CNOT}(c,b)\text{CNOT}(a,b)\text{CNOT}(a,c)$ to move all $(n-1)$ gates $\text{CNOT}(a,c)$ with parameter p_* to the front of the network. Note, that every time commutation rule is used, the gates just change their position and every time the circuit identity is applied we introduce a new gate $\text{CNOT}(a,b)$. However, such a gate can always be commuted to the closest on the left $\text{CNOT}(a,b)$, and this is accounted for by the updates to the i_* gate presence indicator. The circuit gets transformed to the one illustrated in Fig. 4. Parameters i_* are changed through XORing each i_j , $j < \frac{n(n+1)}{2}$ with p_k , for $k < n$ such that q_k is the target of the gate used at step j . The constructed circuit consists of three parts marked I-III in Fig. 4. The skeleton of each of these parts is described by equation (1), which is obvious for parts II and III and requires a short explanation for part I. Divide the skeleton circuit (Fig. 1a) into $(n-1)$ parts with the first containing first $(n-1)$ gates, the second containing next $(n-2)$ gates, and so on, the last, $(n-1)^{\text{st}}$ part containing one last gate. Then, gate G_i for $i = 1..n-1$ from part I of the circuit in Fig. 4 can be matched (via “skeletonization”) to some gate in the i^{th} part of the skeleton circuit SC . Thus, every linear reversible function can be computed as a maximal depth $3(2n-3) = 6n + O(1)$ circuit. Furthermore, since each SWAP-CNOT pair can be rewritten as two CNOTs (Fig. 5) and SWAP requires no more than 3 CNOT gates, the overall depth in terms of CNOTs can be upper bounded by the expression $18n + O(1)$. We note that in some quantum information processing proposals pair CNOT-SWAP can be executed more efficiently than a single CNOT or a single SWAP, such as in [23], Fig. 1. Due to the locality constraint our upper bound has the same asymptotic as a lower bound, and thus our circuits are asymptotically optimal. Using H-C-P-C-P-C-

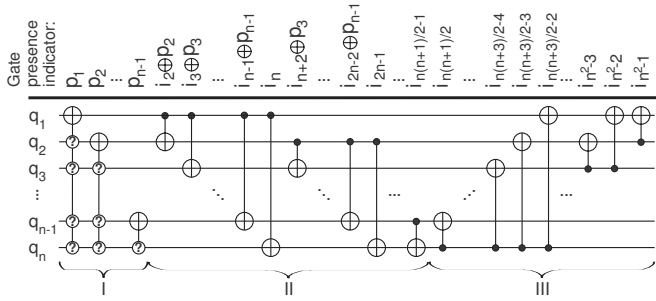


FIG. 4: Gauss-Jordan elimination algorithm network with rearranged gates.

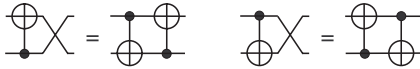


FIG. 5: 2-CNOT circuit equivalent to a SWAP-CNOT pair.

H-P-C-P-C decomposition for stabilizer circuits [20] these upper bounds directly translate to at most depth $30n + O(1)$ circuit composed with generic two-qubit gates, or at most depth $90n + O(1)$ circuit in the library with single-qubit and CNOT gates.

1. Encoding and error syndrome circuits for CSS codes

Encoding and error syndrome circuits for CSS codes are of a great practical importance due to the clever error correcting properties of the CSS codes. Such circuits include those illustrated in Fig. 6(a) (encoding; [24]) and Fig. 6(b) (error syndrome; [5]), where single-qubit Hadamard gates are not illustrated since their contribution to the total depth is only a constant, and the controlled gates, each of which may or may not be present (which is defined by the form of the parity check matrices of the corresponding classical codes), are either controlled-NOT or controlled-Z. Our circuit parallelization technique described in the previous subsection applies directly to such circuits since each of them has skeleton as described by the Eq. (1) with $n = s + t + 1$ for the encoding circuit and $n = s + t$ for the error syndrome circuit. This allows us to execute the encoding circuit in $(2s + 2t - 1)$ stages and the error syndrome circuit in $(2s + 2t - 3)$ (in both cases, $s, t \geq 1$) stages composed of generic two-qubit gates. However, a better approach is possible. The following construction is, essentially, a part of the algorithm used to execute SC .

Consider encoding circuit (Fig. 6(a)). Prepare the qubits in the following LNN connectivity pattern $a_1 - a_2 - \dots - a_s - b - c_t - c_{t-1} - \dots - c_1$. At each level i apply gates whose targets intersect with the sloping lines marked “level i ” shown in Fig. 6(a). Each such level is followed by the level of SWAPs applied to the same qubits as the gates from the previous level to allow for the next set of gates to get executed in the LNN architecture. For example, for $s = 3$ and $t = 4$

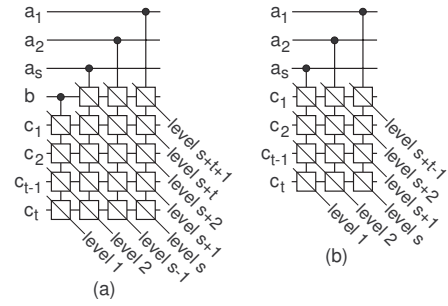


FIG. 6: General structure of the (a) encoding and (b) syndrome detection circuits for CSS quantum error correcting codes.

level 3 will be composed of the gates $G(b, c_2)$, $G(a_3, c_3)$, and $G(a_2, c_4)$, followed by the swaps $SWAP(b, c_2)$, $SWAP(a_3, c_3)$, and $SWAP(a_2, c_4)$. Thus, the total depth of the encoding circuit executable in the LNN architecture will be equal to $(s + t + 1)$ if it is allowed to be composed of generic two-qubit gates. This is almost half of what was expected if this circuit were matched to the SC first. This translates to a depth $2(s + t + 1)$ circuit with controlled-NOT, controlled-Z and SWAP gates. Similarly, the depth of the error syndrome circuit composed with generic gates and executable in the LNN architecture is $(s + t - 1)$.

Application of the technique described in this subsection to executing the error syndrome circuit for Steane’s code ([5], Fig. 10.16) in the LNN architecture shows that this can be done in 12 stages composed of generic two-qubit gates or $26 (= 2 * 12 + 2)$ stages composed of Hadamard, controlled-NOT, controlled-Z, and SWAP gates. We can show that the encoding circuit of [24], Fig. 8b, can be executed in 23 stages composed of generic two-qubit gates or, alternatively, $68 (= 3 * 23 + 1 - 2)$: pairs CNOT-SWAP must be combined, we need an extra level for Hadamard gates, but do not need to apply last SWAP) stages composed of CNOT and Hadamard gates in the LNN architecture. Our result for the depth, 68, is notably better than 177 found by the automated procedure of [24].

III. LOWER BOUNDS

In this section we study lower bounds on the depth of skeleton circuit SC defined in equation (1) assuming all gates are present (*i.e.*, each $i_* = 1$). We further assume that a pair of gates $G(q_i, q_j)SWAP(q_i, q_j)$ requires two units of the execution time, one for each of the gates. In practice, a direct implementation of pair $G(q_i, q_j)SWAP(q_i, q_j)$ may be more efficient [6], but the particulars of such a construction depend on the specific Hamiltonian, which is unknown in the general case. The depth of circuit illustrated in Fig. 1(c) is thus $(4n - 6)$. The lower bounds achieved below are directly applicable to the QFT circuit.

To prove lower bounds, we need to restrict the set of possible computations. We define two circuit type quantum com-

putational models A and B . We require that for each of them in order to compute the SC (equation (1)) all $\frac{n(n-1)}{2}$ two-qubit gates need to be executed, and no ancilla qubits may be used. Furthermore,

- in model A we assume that the gates required to be executed in SC cannot be commuted (other than trivially—a pair of gates operating on non-intersecting sets of qubits always commutes);
- in model B we allow possibility of the execution of gates in any order (*i.e.*, this lets us obtain bounds that allow commuting gates through the circuit, without worrying about which gates actually commute, and what kind of corrections are needed in case they do not commute).

The architectures considered in this paper are LNN , $2D$ square lattice, and $bounded$ degree graph with the degree of each vertex no more than k . We next prove a number of lower bounds, refer to Table I.

TABLE I: Lower bounds on the depth of the SC in models A and B in the LNN , $2D$ square lattice, and $bounded$ degree graph architectures.

	LNN	$2D$ square lattice	$bounded$ degree graph
model A	$\frac{10n}{3} + O(1)$	$3n + O(1)$	$(2 + \frac{2}{k})n + O(1)$
model B	$\frac{3n}{2} + O(1)$	$\frac{5n}{4} + O(1)$	$(1 + \frac{1}{k})n + O(1)$

$\frac{10n}{3} + O(1)$ **bound in LNN, model A.** First, denote each depth-1 computational stage (logic level) by L and each depth-1 swapping stage by S . Every three stages of the SC have a single fixed qubit that interacts with three other qubits. This is either q_1, q_2 , or q_n . Thus, every three logic levels have to be separated by a round of SWAPs, each having depth at least 1, *i.e.* each sequence LLL must be replaced by $LSLL$ or $LLSL$ to be able to run the circuit in the LNN architecture. We call this $3L \rightarrow 1S$ requirement. With the $3L \rightarrow 1S$ requirement, the total depth must be at least $2n - 3 + \lceil \frac{1}{2}(2n - 5) \rceil = 3n + O(1)$ logic levels. Therefore, using just the $3L \rightarrow 1S$ requirement proves that our circuit is at most factor $\frac{4}{3}$ off the optimum. We now improve this bound to $\frac{10n}{3} + O(1)$ by showing that every 4 computational stages must be separated by at least depth-2 swapping stage ($4L \rightarrow 2S$ requirement). $4L \rightarrow 2S$ is slightly more restrictive than $3L \rightarrow 1S$. The difference between the two is that in one $LLSLL$ is allowed, but not in the other. We next prove that depth-1 level does not suffice in separating some two computational stages from the following two by exploring the properties of SC and the LNN architecture.

Assume all 4 computational stages L_i, L_{i+1}, L_{i+2} , and L_{i+3} are solely in the first half of SC . The second half is symmetric to the first half and thus a similar proof holds for it. We do not prove the boundary case (where one part of the 4-stage computation is in the first half of the SC and the other part is in the second half) because its contribution to the final figure is only a constant. Next, assume i is odd. The proof for even values i is analogous. Name the qubits q_1, q_2, \dots, q_n top to bottom. The computational stages L_i and L_{i+1} use

interactions $q_{i+2} - q_1, q_1 - q_{i+1}, q_{i+1} - q_2, \dots, q_{i+1} - q_{i+3}$, which in the LNN architecture can only be aligned as follows: $q_{i+2} - q_1 - q_{i+1} - q_2 - \dots - q_{i+1} - q_{i+3}$. The computational stages L_{i+2} and L_{i+3} use interactions $q_{i+4} - q_1, q_1 - q_{i+3}, q_{i+3} - q_2, \dots, q_{i+3} - q_{i+5}$. In particular, stages L_{i+2} and L_{i+3} require interaction $q_{i+3} - q_{i+7}$, and qubit q_{i+7} is used both in L_{i+2} and L_{i+3} . However, we know that after completion of stages L_i and L_{i+1} , the architecture allows interactions in the following order $q_{i+3} - q_{i+1} - q_{i+5} - q_{i-1} - q_{i+7}$. The LNN architecture distance between q_{i+3} and q_{i+7} is 4. A depth-1 swapping reduces the architectural distance between these qubits by at most 2, which is not enough for the desired interaction to be allowed. Thus, the depth of swapping must be at least 2. This concludes the proof of the $4L \rightarrow 2S$ requirement.

We finalize the proof of $\frac{10n}{3} + O(1)$ lower bound by observing that for a circuit with $2n + O(1)$ stages L we need to have at least $\frac{4n}{3} + O(1)$ stages S to satisfy $4L \rightarrow 2S$ requirement. Thus, the total number of stages required to execute SC in LNN is $\frac{10n}{3} + O(1)$. This implies that the circuit we constructed explicitly (Fig. 1(c)) must be within factor of $\frac{6}{5}$ from optimum.

$3n + O(1)$ **lower bound in 2D square lattice, model A.** We prove that every three computational stages L_{i-2}, L_{i-1} , and L_i , where $i = 2k + 1$ and $k = 1.. \lceil \frac{n-2}{2} \rceil$ (this means that all computational stages are in the first part of SC ; the proof for the symmetric second part is similar) must contain at least one swapping stage if ran in 2D square lattice architecture. We prove this by finding three interactions that form a loop. Vertices in such loop cannot be isomorphically mapped to the vertices of 2D square lattice. The interactions that form such a loop, assuming qubits are named q_1, q_2, \dots, q_n top to bottom, are $q_{i-1} - q_{i+1}$ in L_{i-2} , $q_{i-1} - q_{i+3}$ in L_{i-1} , and $q_{i+1} - q_{i+3}$ in L_i . This proves that for every possible value k it is required to have at least one swapping stage, which results in the construction of $3n + O(1)$ lower bound.

The lower bound that we just proved may be interesting to those experimentalists working on implementing 2D architectures for quantum information processing. The lower bound shows that, with certain restrictions, the QFT in 2D square lattices cannot in principle be parallelized any more efficiently than to a depth at least $\frac{3}{4}$ of the depth of QFT circuit executable in the LNN architecture.

$\frac{3n}{2} + O(1)$ **lower bound in NCT, model B.** Recall that the number of gates in SC is $\frac{n(n-1)}{2}$ and they all require different qubit-to-qubit interactions to be available. Next, note that in the LNN architecture application of a single SWAP may make at most two new interactions become available for a gate to be applied on. Thus, the total number of SWAPs that one must execute in a circuit to go through all $\frac{n(n-1)}{2}$ possible interactions is at least $\lceil \frac{\frac{n(n-1)}{2} - (n-1)}{2} \rceil = \lceil \frac{(n-1)(n-2)}{4} \rceil$. This means that the total number of gates to be executed in the LNN architecture to compute SC must be at least $\frac{n(n-1)}{2} + \lceil \frac{(n-1)(n-2)}{4} \rceil = \lceil \frac{(3n-2)(n-1)}{4} \rceil$. At most $\lfloor \frac{n}{2} \rfloor$ gates can be executed in paral-

lel. Thus, the depth of the circuit is at least the minimum total number of gates to be executed divided by the maximum number of gates that can be executed simultaneously, *i.e.* $\frac{3n}{2} + O(1)$.

This lower bound is constructed based on the assumption that all gates in SC need to be executed, and does not take into account that the order they are executed in is important. Thus, the restriction on the form of the computation is significantly weaker than that for model A , and the proven lower bound is looser.

Generalizing the above techniques, it can be shown that in an architecture where each qubit has a finite number of neighbors bounded by number k :

- the lower bound for executing SC is $(2 + \frac{2}{k})n + O(1)$ in model A ;
- the lower bound for executing SC is $(1 + \frac{1}{k})n + O(1)$ in model B .

The $\frac{5n}{4} + O(1)$ lower bound announced in Table I follows from the second of these two statements. Given the linearity of proven lower and upper bounds, we have just shown the asymptotic optimality of the depth of our skeleton circuit in the restricted architectures considered in this paper.

IV. CONCLUSION

In this paper we studied the complexity of the execution of the quantum Fourier transformation and stabilizer circuits in restricted architectures.

We reconstructed the depth $4n + O(1)$ circuit (composed with SWAP and controlled- Z gates) for QFT initially reported in [17] which is implemented in the LNN architecture. With

the application of our generalized technique we showed how the approximate QFT circuit can be executed in linear depth in the LNN architecture. We proved a number of lower bounds for the depth of QFT circuit, which are all a constant factor away (ranging from $\frac{1}{4}$ to $\frac{5}{6}$, and depending on the computational model and assumptions made) from the above upper bound. Some of our lower bounds can be used by experimentalists working on implementing advanced architectures as a guide to how complex architectures may need to be for particular types of computations. For instance, we proved that, with certain restrictions, the QFT circuit in 2D square lattices cannot in principle be parallelized more than to the depth equal to $\frac{3}{4}$ of the depth of QFT circuit executable in the LNN architecture.

More importantly, we presented a constructive algorithm for synthesizing linear depth stabilizer circuits in the LNN architecture. In particular, we showed that any stabilizer circuit can be executed in at most $30n + O(1)$ stages each composed with generic two-qubit gates, which in the library with CNOT and single-qubit gates translates to at most depth $90n + O(1)$ circuit. This upper bound is asymptotically optimal. We considered specific stabilizer circuits and showed how these circuits can be executed faster than reported by previous researchers [24].

Acknowledgments

I would like to thank Prof. Michele Mosca from the University of Waterloo and for his help in preparation of this manuscript and useful discussions. I wish to thank Jacob D. Biamonte from the University of Oxford and Donny Cheung from the University of Waterloo for their help in preparation and proofreading this manuscript. This work was supported by PDF grant from the National Sciences and Engineering Research Council of Canada.

-
- [1] L. K. Grover. A fast quantum mechanical algorithm for database search. Proceedings of 28th Annual ACM Symposium on the Theory of Computing, pages 212-219, 1996, quant-ph/9605043.
 - [2] P. W. Shor. Polynomial-time algorithms for prime factorization and discrete logarithms on a quantum computer. *SIAM Journal of Computing*, 26:1484–1509, 1997, quant-ph/9508027.
 - [3] C. Negrevergne, T. S. Mahesh, C. A. Ryan, M. Ditty, F. Cyr-Racine, W. Power, N. Boulant, T. Havel, D. G. Cory, and R. Laflamme. Benchmarking quantum control methods on a 12-qubit system. *Physical Review Letters*, 96(170501), 2006, quant-ph/0603248.
 - [4] H. Häffner, W. Hänsel, C. F. Roos, J. Benhelm, D. Chek-al-kar, M. Chwalla, T. Körber, U. D. Rapol, M. Riebe, P. O. Schmidt, C. Becher, O. Gühne, W. Dür, and R. Blatt. Scalable multiparticle entanglement of trapped ions. *Nature* 438:643–646, December 2005, quant-ph/0603217.
 - [5] M. Nielsen and I. Chuang. *Quantum Computation and Quantum Information*. Cambridge University Press, 2000.
 - [6] J. Zhang, J. Vala, S. Sastry, and K. B. Whaley. Geometric theory of nonlocal two-qubit operations. *Physical Review A*, 67(042313), 2003, quant-ph/0209120.
 - [7] L. M. K. Vandersypen, M. Steffen, G. Breyta, C. S. Yannoni, M. H. Sherwood, and I. L. Chuang. Experimental realization of Shor’s quantum factoring algorithm using Nuclear Magnetic Resonance, *Nature* 414:883–887, December 2001.
 - [8] R. Van Meter and M. Oskin. Architectural implications of quantum computing technologies. *ACM Journal on Emerging Technologies in Computing Systems*, 2(1):31–63, 2006.
 - [9] D. Copley, M. Oskin, F. Impens, T. Metodiev, A. Cross, F. T. Chong, I. L. Chuang, and J. Kubiatiowicz. Toward a scalable silicon-based quantum computing architecture. *IEEE Journal of Selected Topics in Quantum Electronics*, 9(6):1552–1569, 2003.
 - [10] A. Skinner, M. Davenport, and B. Kane. Hydrogenic spin quantum computing in silicon: a digital approach. *Physical Review Letters*, 90(087901), 2003, quant-ph/0206159.
 - [11] J. Sherson, H. Krauter, R. K. Olsson, B. Julsgaard, K. Hammerer, I. Cirac, E. S. Polzik. Quantum teleportation between light and matter. *Nature* 443:557–560, 2006.
 - [12] G. Burkard and A. Imamoglu. Ultra-long distance interaction between spin qubits. *Physical Review B* 74(041307), 2006,

- cond-mat/0603119.
- [13] A. M. Steane and D. M. Lukas. Quantum computing with trapped ions, atoms and light. *Fortschritte der Physik*, 48(9-11):839–858, 2000, quant-ph/0004053.
- [14] R. Cleve and J. Watrous. Fast parallel circuits for the quantum Fourier transform. In *IEEE Symposium on Foundations of Computer Science*, pages 526–536, 2000, quant-ph/0006004.
- [15] D. Coppersmith. An approximate Fourier transform useful in quantum factoring. Technical Report RC19642, IBM, 1994.
- [16] C. Moore and M. Nilsson. Parallel quantum computation and quantum codes, 1998, quant-ph/9808027.
- [17] A. G. Fowler, S. J. Devitt, and L. C. L. Hollenberg. Implementation of Shor’s algorithm on a linear nearest neighbor qubit array. *Quantum Information and Computation*, 4(4):237–251, 2004, quant-ph/0402196.
- [18] C. H. Bennett, D. P. DiVincenzo, J. A. Smolin, and W. K. Wootters. Mixed-state entanglement and quantum error correction. *Physical Review A*, 54(3824), 1996, quant-ph/9604024.
- [19] D. Gottesman. A class of quantum error-correcting codes saturating the quantum Hamming bound. *Physical Review A* 54(1862), 1996, quant-ph/9604038.
- [20] S. Aaronson and D. Gottesman. Improved simulation of stabilizer circuits. *Physical Review A*, 70(052328), 2004, quant-ph/0406196.
- [21] A. Broadbent and E. Kashefi. Parallelizing Quantum Circuits, April 2007, arXiv:0704.1736.
- [22] K. N. Patel, I. L. Markov and J. P. Hayes. Efficient synthesis of linear reversible circuits. In *International Workshop on Logic Synthesis*, Temecula Creek CA, June 2004, pp. 470-477, quant-ph/0302002.
- [23] A. G. Fowler, C. D. Hill and L. C. L. Hollenberg. Quantum error correction on linear nearest neighbor qubit arrays. *Physical Review A*, 69(042314), 2004, quant-ph/0311116.
- [24] T. Metodi, D. D. Thaker, A. W. Cross, F. T. Chong, and I. L. Chuang. Scheduling physical operations in a quantum information processor. In *Proceedings of the SPIE*, Volume 6244, pp. 62440T, 2006.